Romanian Reports in Physics, Vol. 68, No. 2, P. 642–647, 2016

HIGH EFFICIENCY MATERIALS BASED ON Ge FOR HIGH SPEED DEVICES

I. GRUIA

Faculty of Physics, University of Bucharest, Romania,
E-mail: gruia_ion@yahoo.com

Received April 12, 2015

Abstract. In this paper, we present results and discussions concerning photoelectrical characterization and time response of Ge-nanocrystals (Ge-ncs) embedded in SiO_2 insulating matrix. The investigated Al/Si/$GeSiO_2$/ITO sandwich structure has high internal quantum efficiency (IQE) in the 700÷1100 nm wavelength range, peak responsivity approaching 2 A/W when illuminated in the VIS and NIR wavelength range and also a short time response.

Key words: Al/Si/$GeSiO_2$/ITO structures, Ge diffusion, Ge nanocrystals formation.

1. INTRODUCTION

Over the last few decades, nanostructured materials and nanostructures have attracted much attention in prestigious research laboratories due to their optical and electrical properties suited for multiple technological applications. Germanium is one of the important semiconductors which can be used as a sensitive photo detector in the infrared region. Nanostructured Ge, compared with Si, present a stronger confinement effect due to its larger excitonic Bohr radius (Ge~24.3 nm and Si~4.9 nm) [1, 2] and higher Hall mobility of carriers, about 4 times larger than for Si. Moreover, since the electronic band gap of bulk Ge (0,66eV) is much lower that of bulk Si (1,1eV). Other advantage is more convenient preparation conditions like lower crystallization temperature that avoid Ge diffusion [3]. Ge-ncs embedded in to various insulating matrices are interesting for their potential application in optoelectronic devices [4], photo detectors [5], light emitters [6], memory devices [7] and solar cells [8, 9]. It has been demonstrated that Ge-ncs (Ge-nanocristals) incorporated into a SiO_2 matrix are photo-sensitive structures in the visible or infrared range due to the quantum confinement effect [10] or due to carrier traps located at the interface between Ge-ncs and the surrounding SiO_2 matrix [11–13].

Concerning the deposition method to realize Ge-ncs embedded in to SiO_2 matrix, sputtering [14], ion implantation [15] or thermal evaporation [16] they may

suffer from issues related to the ease of controlling the deposition parameters and/or the extent of inevitable defects [12–19].

In this paper, we present results and discussions concerning photoelectrical characterization and time response of Ge-nps (Ge-nanoparticles) embedded in SiO_2 insulating matrix. The nanostructures prepared by magnetron sputtering show superior photo-responsivity and large operation bandwidth. More significantly, these materials may be employed individually or in connection with other III–V compound semiconductors, as GaAs and GaSb, thus opening the way to new opportunities for fabricating various types of hybrid heterojunctions on Si.

2. EXPERIMENTAL

The samples investigated in this paper are schematically presented in Fig. 1. These samples are prepared in NIMP (National Institute of Materials Physics) and preparation conditions are presented and described in detail in Ref. [17–21].

The active films of Ge-nps embedded in SiO_2 matrix were prepared by co-sputtering of Ge and SiO_2 on clean square substrates of n-type (100) Si maintained at 300 °C during deposition. The samples, with sandwich geometry, have electrodes of ITO (top one) with 3×3 mm^2 size and of Al (bottom one).

The SiGeO films have 0.25 μm thickness. We characterized the photocurrent response time of the structure compared to Thorlabs PDA10CS-EC InGaAs PIN Amplified Detector. Measurements were performed under normal incidence illumination of a $\lambda = 808.5$ nm laser beam, modulated by a mechanical chopper at $f = 3$ KHz and the signal was recorded by a Digital Oscilloscope model LeCroy WaveJet 332.

The spectral responsivity characteristics were recorded (at NIMP) at room temperature using a set-up containing an optical cryostat, an electrometer with voltage source included, a temperature controller, a monochromator and a mechanical chopper.

3. RESULTS AND DISCUSSIONS

A drawing of studied structures is shown in Fig. 1 and additional fabrication details are presented in the cross-section in Fig. 2 (SEM images).

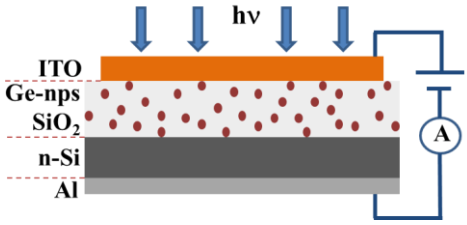

Fig. 1 – Nanostructure configuration and measurement setup schematically.

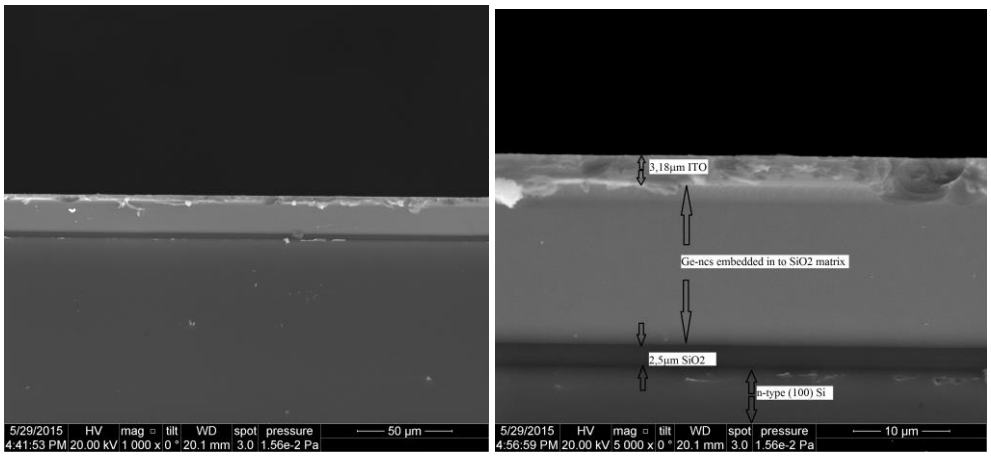

Fig. 2 – Different SEM images of the structure (cross section) which shows the Ge layers for the multilayered structure thickness.

Figure 3(a) shows the spectral responsivity defined in eq. (1) as the ratio between the photogenerated current $(I_{light} - I_{dark})$ and the incident optical power $(P_{opt.})$:

$$R_{sp} = \frac{I_{light} - I_{dark}}{P_{opt.}}. \tag{1}$$

The internal quantum efficiency (IQE) defined as the number of photo-generated carriers divided by the number of absorbed photons, is calculated from Fig. 3(c) using the following equation:

$$\mathrm{IQE} = \frac{100 \cdot h \cdot c \cdot I(\lambda)}{e \cdot \lambda \cdot P_{opt.}(\lambda)}, \tag{2}$$

were: e is the elementary charge, h is Planck's constant, c is the speed of light in vacuum, $I(\lambda)$ is photogenerated current and $P_{opt.}(\lambda)$ is the incident optical power. The measurements were performed at three different values of reverse bias of 0.1 V, 0.5 V and 1 V respectively.

The peak IQE observed is as high as 350 % at λ = 980 nm and reverse bias of 1 V. These results tell us that for each absorbed incident photons are generated at least two carriers (leading to carrier multiplication).

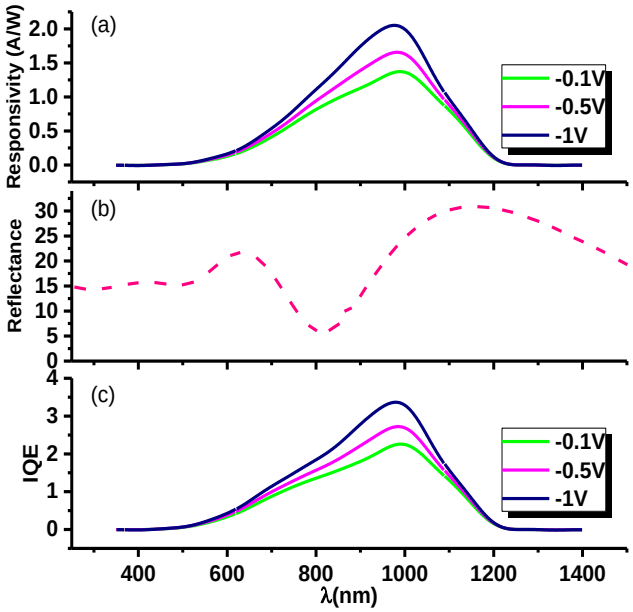

Fig. 3 – a) Spectral responsivity of the investigated structure obtained at various applied reverse bias; b) measured reflectance spectra as a function of excitation wavelength in the range of 350 ÷ 1400 nm; c) internal quantum efficiency (IQE) as a function of wavelength under different reverse bias values.

To further understand the behaviour of the structure, we performed transient photo response experiments. The device was illuminated with a laser beam (λ = 808.5 nm) chopped mechanically at 3 kHz. This measurement was performed without bias, so that there is no electron injection into the ITO layer, only photon absorption in Ge-ncs, slow tunnelling transport at holes and also photon absorption in the silicon substrate. The photon absorption leads to transitions between the extended electronic states from the valence band toward the conduction band. The light absorption in Ge-ncs embedded in SiO_2 is strongly influenced by the surface of Ge-ncs. One can observe a feature at about 1140 nm peak, probably correlated to Ge-ncs (optical transition for $\Delta l = 1$, between energy levels $|0,2> \rightarrow |1,1>$ where $|n,l>$ is the quantum confinement in Ge-ncs, n-radial quantum number and l-orbital quantum number) [22, 23]. The shoulder located about 730 nm is more probably related to the Ge-ncs/SiO_2 interface states than to Ge-ncs. The photon absorption seems to be mediated by surface electronic states, not related to the volume of Ge-ncs.

From the time-resolved measurements reported in Fig. 4, we presented the results of a study dedicated to optimization of preparation process and photoelectrical characterization of Ge-ncs embedded in SiO_2 thin film insulator.

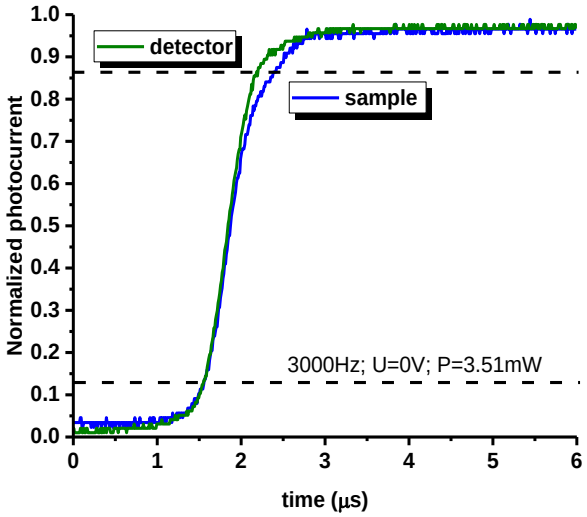

Fig. 4 – Normalized photocurrent response time characteristics. The green line represents the baseline system response (~0.6 μs response time) obtained under illumination using a λ = 808.5 nm laser beam modulated by a mechanical chopper at *f* = 3 KHz using a commercial InGaAsP photodiode. With blue line is represented the structure photoresponse signal (~0.8 μs response time).

4. CONCLUSIONS

Deposition of thin films was realized by magnetron sputtering on Si substrate heated at 300°C. We have demonstrated that investigated Al/Si/GeSiO$_2$/ITO sandwich structure show a high internal quantum efficiency (IQE = 350 %) in the 700÷1100 nm wavelength range, as well as peak responsivity approaching 2 A/W when illuminated in the VIS and NIR wavelength range and also a high time response. Finally, light to current conversion in photodetector structures based on Ge nanocrystals has been investigated, showing that Ge-ncs in SiO$_2$ provide significant photoresponse. These structures provide major advantages compared to the existing devices, as they can be operated at reverse bias as low as 1 V and can be fabricated with common processing operations at temperature below 300 °C. We attribute their high efficiency to photoconductive gain provided by the trapping of holes in the Ge-ncs. These findings open a route toward the realization of high-efficiency photodetectors based on Ge-ncs which can be easily integrated into a standard silicon complementary metal-oxide semiconductor process.

Acknowledgements. The author would like to thank Dr. C. Luculescu from the National Institute for Laser, Plasma & Radiation Physics (INFLPR) for the SEM measurements and Dr. I. Stavarache from Group of Si-and Ge-band nanomaterials and nanostructures from NIMP for samples preparation and photocurrent measurements.

REFERENCES

1. W. Kohn, J. M. Luttinger, Phys. Rev. **98**, 915 (1955).
2. G. Gu, M. Burghard, G. T. Kim, G. S. Düsberg, P. W. Chiu, V. Krstic, S. Roth, W. Q. Han, J. Appl. Phys. **90**, *11*, 5747 (2001).
3. A. A. Shklyaev, K. N. Romanyuk, A. V. Latyshev, Journal of Surface Engineered Materials and Advanced Technology **3**, 195 (2013).
4. Ali K. Okyay, DuyguKuzum, Salman Latif, David A. B. Miller, and Krishna C. Saraswat, IEEE Transaction on Electron Devices **54**, 3252 (2007).
5. L. Chen, M. Lipson, Optics Express **17**, 10, 7901 (2009).
6. J. R. Jain, A. Hryciw, T. M. Baer, D. A. B. Miller, M. L. Brongersma, R. T. Howe, Nature Photonics **6**, 398 (2012).
7. S. K. Ray, S. Maikap, W. Banerjee, and S. Das, J. Phys. D: Appl. Phys. **46**, 153001 (2013).
8. Y. Wanga, A. Gerger, A. Lochtefeld, L. Wanga, C. Kerestes, R. Opila, A. Barnett, Solar Energy Materials & Solar Cells **108**, 146 (2013).
9. T. Tayagaki, Y. Hoshi, N. Usami, Scientific Reports **3**, 3225 (2013).
10. S. S. Tzeng and P. W. Li, Nanotechnology **19**, 235203 (2008).
11. S. Cosentino, S. Mirabella, Pei Liu, Son T. Le, M. Miritello, S. Lee, I. Crupi, G. Nicotra, C. Spinella, D. Paine, A. Terrasi, A. Zaslavsky, D. Pacifici, Thin Solid Films **548**, 551 (2013).
12. I. Stavarache, M. L. Ciurea, Journal of Optoelectronics and Advanced Materials **9**, *8*, 2644 (2007).
13. V. Iancu, M. L. Ciurea, I. Stavarache, V. S. Teodorescu, Journal of Optoelectronics and Advanced Materials **9**, *8*, 2638 (2007).
14. O. Wolf, I. Balberg, O. Millo, Thin Solid Films **574**, 184 (2015).
15. J. Y. Zhang, Y. H. Ye, X. L. Tan, Appl. Phys. Lett. **74**, *17*, 2459 (1999).
16. G. Masini, V. Cencelli, L. Colace, F. De Notaristefani, G. Assanto, Physica E **16**, 614 (2003).
17. I. Stavarache, A. M. Lepadatu, T. Stoica, M. L. Ciurea, Applied Surface Science **285P**, 175 (2013).
18. A. M. Lepadatu, T. Stoica, I. Stavarache, V. S. Teodorescu, D. Buca, M. L. Ciurea, J. Nanopart. Res. **15**,1981 (2013).
19. A. M. Lepadatu, I. Stavarache, T. F. Stoica, M. L. Ciurea, Digest Journal of Nanomaterials and Biostructures **6**, *1*, 67 (2011).
20. I. Stavarache, A. M. Lepadatu, A. V. Maraloiu, V. S. Teodorescu, M. L. Ciurea, J. Nanopart. Res. **14**, 930 (2012).
21. I. Stavarache, A. M. Lepadatu, N. G. Gheorghe, R. M. Costescu, G. E. Stan, D. Marcov, A. Slav, G. Iordache, T. F. Stoica, V. Iancu, V. S. Teodorescu, C. M. Teodorescu, M. L. Ciurea, J. Nanopart. Res. **13**, 221 (2011).
22. A. M. Lepadatu, I. Stavarache, M. L. Ciurea, V. Iancu, J. Appl. Phys. **107**, 033721 (2010).
23. V. Iancu, M. R. Mitroi, A. M. Lepadatu, I. Stavarache, M. L. Ciurea, J. Nanopart. Res. **13**, 1605 (2011).